Iranian Journal of Catalysis 10(2), 2020, 127-134

IRANIAN JOURNAL OF CATALYSIS

The performance of $NiMo/SiO_2$-Al_2O_3 and $NiMo/SO_4$-Al_2O_3 catalysts for hydrocracking of n-hexadecane

Ehsan Taghizadeh Yusefabad[a], Ahmad Tavasoli[a,*], Yahya Zamani[b]

[a]*School of Chemistry, College of Science, University of Tehran, Tehran, Iran.*

[b]*Research Institute of Petroleum Industry (RIPI), Tehran, Iran.*

Received 25 January 2019; received in revised form 20 April 2019; accepted 6 May 2019

ABSTRACT

In this study, the performance of NiMo catalysts over an amorphous SiO_2-Al_2O_3 and SO_4-Al_2O_3 with various contents of H_2SO_4 was investigated for the n-hexadecane hydrocracking (n-C_{16}) using a down flow fixed bed micro-reactor. The synthesized catalysts were characterized using BET, XRD, and NH_3-TPD analysis. The analysis of the coke formed on the catalysts has been carried out using the TG-TPO. The obtained results indicated that the coke formation was decreased by increasing sulfuric acid content in catalysts. The performance of the catalysts was investigated for n-C_{16} hydrocracking and the liquid products were analyzed using GC-MS. The catalytic activity increased when sulfuric acid content increased and reached to about 99% conversion using catalyst containing 0.21 wt.% H_2SO_4.

***Keywords**: Molybdenum, Nickle, Catalyst, Hydrocracking, Sulfuric acid.*

1. Introduction

The interest for heavy crude oils is increased with respect to the growing worldwide energy demand. However, the quality of crude oil was decreased and the petroleum sources have been changed into heavy and extra-heavy crude oils [1,2]. These heavy crude oils have high contents of residue in the bottom of the barrel in which their *fractional distillation* resulted in the lower amounts of distillates with the large investment in distillation plants [3]. Also, the conversion of residues (e.g., Vacuum Gas Oil (VGO)) into the valuable distillates (e.g., gasoline and diesel) is an important factor for the sustainability and profitability of oil refineries [2]. Therefore, it is necessary to convert the large molecules into low molecular weight fractions (middle distillates and gasoline) and to remove their impurities such as sulfur, nitrogen and metals [1].

There are several processes for converting the residues such as viscosity reduction, solvent extraction, gasification, coking and hydrocracking [4,5]. In the coking process, the heavy paraffinic, naphthenic and malthenic hydrocarbons have been transformed into the light hydrocarbons via the thermal cracking; while the asphaltenic hydrocarbons have been mainly transformed into the coke via the polycondensation reactions. One of the drawbacks of this process is the low quality of the products with high contents of olefins, sulfur, nitrogen and aromatics which need further treatment for commercial specifications [6].

The catalytic hydrocracking process converts the heavy hydrocarbons such as asphaltenes into the light distillates without the impurities such as nitrogen, sulfur and olefins. The hydrocracking products require the post-treatment to meet the commercial specifications. However, the severity of this method is lower than that of the products of the coking technique. The main advantages of the coking process over the hydrocracking method are the lower investment and operating costs (Initial cost). However, considering the costs of post-treatment and the yields of valuable products, the hydrocracking process has been preferred [4,5,7,8].

The main problem in the hydrocracking process was the fast deactivation of the used catalyst during the hydrocracking process and following the high consumption of the catalyst.

*Corresponding author.
E-mail address: tavasoli.a@ut.ac.ir (A. Tavasoli)

The supply of fresh catalyst and the disposal of the wasted catalyst due to the environmental regulations may become very complicated. Moreover, the price of the catalysts produced from molybdenum, nickel, cobalt and tungsten supported on alumina has risen to 300% in the last 10 years; this limits the advantage of this technique [4,9]. To overcome this problem, the synthesis of bi-functional catalysts over a support has been proposed [4]. The combination of properties of silica and alumina oxides as a support could have a positive impact on the hydrocracking of heavy oil using catalysts [1]. The various studies have been reported for the catalytic hydrocracking of heavy oil into the middle distillates [1,10,11]. However, there is a small number of studies about the effect of sulfide phase of support on the heavy oil hydrocracking, especially the hydrocracking of heavy crude oil with the high content of asphaltenes as a feedstock. Ferraz *et al.* studied the effect of the support acidity of NiMo sulfided catalysts for hydrogenation and hydrocracking [12] and investigated the effect of the support acidity on the overall activity and products distribution. In another study, the influence of support acidity on the activity of catalysts for hydrogenation and hydrocracking of NiMoS catalysts was evaluated [13]. They found that the hydrogenation activity of sulfided catalysts can be modified by neighboring acidic sites. Dik *et al.* [6] investigated the composition of stacked bed for VGO hydrocracking with maximum diesel yield. They found that the maximum selectivity to diesel and the highest diesel yield were achieved using the NiMo /ASA-Al_2O_3 catalyst [6].

In this study, four bi-functional catalysts containing the NiMo over an amorphous ASA- Al_2O_3 and three Al_2O_3-SO_4/Al_2O_3 supports containing 0.07 wt.%, 0.14 wt.%, and 0.21wt.% H_2SO_4 have been synthesized and their application was investigated for the n-hexadecane (n-C_{16}) hydrocracking. The synthesized catalysts were characterized using Brunauer–Emmett–Teller (BET), X-ray diffraction (XRD), and NH_3 temperature programmed desorption (NH3-TPD). The quantitative analysis of the coke formed on the catalyst surface has been carried out using the thermo-gravimetric-temperature-programmed oxidation (TG-TPO) method. The performance of the catalysts was investigated for n-C_{16} hydrocracking and the final liquid products were analyzed using GC-MS.

2. Experimental

2.1. Materials

Alumina (Al_2O_3) granules, silica, ammonium heptamolybdate, nickel nitrate and n-hexadecane (as a feedstock) were purchased from Merck (Darmstadt Germany).

2.2. Synthesis of supports

The ASA-Al_2O_3 support was prepared according to the following method. The support contains 70% Al_2O_3-SiO_2 and 30% γ-Al_2O_3. Al_2O_3-SiO_2 is composed of 10 wt.% γ-Al_2O_3 and 90 wt.% SiO_2. The obtained mixture was loaded into the mixer equipped with Z-folded blades. Then the mixture was pepticized into the nitric acid under stirring for 30 min. The obtained paste was extruded using the plunger extruder VINCI with a Teflon spinneret containing trilobular holes at a pressure of 3.5–4.0 MPa and a velocity of plunger moving of 1.2 mm/s. The extruded mixture was dried for 4 h at 120 ℃ in air flow and then heated for 2 h to 415 ℃ followed by calcining at 415 ℃ for 4 h. Then 30% of γ-Al2O3 was added to the above mixture. The powder mixture was loaded into a mixer with Z-folded blades. Extrudates were dried for 2 h at 120 ℃ in air flow and then heated for 2 h to 415 ℃ and calcined at 415 ℃ for 4 h.

Three (Al_2O_3-SO_4)-Al_2O_3 supports were prepared according to the following method. The support contains 70% of Al_2O_3-SO_4 and 30% of γ-Al_2O_3. Al_2O_3-SO_4 supports were composed of γ-Al_2O_3, and 0.07 wt.%, 0.14 wt.%, and 0.21 wt.% H_2SO_4. The obtained mixtures were dried for 2 h at 120 ℃ in air flow and then heated to 415 ℃ and then calcined at 415 ℃ for 4 h. Then 30% of γ-Al_2O_3 was added to the above mixture. The mixture of powder was loaded into a mixer with Z-folded blades and stirred for 30 min. Then, it was extruded using plunger extruder VINCI with a Teflon spinneret at a pressure of 3.5–4.0 MPa and a velocity of plunger moving of 1.2 mm/s. Finally, the extrudates were dried for 2 h at 120 ℃ in air flow and then heated for 2 h to 415 ℃ and calcined at 415 ℃ for 4 h.

2.3. Synthesis of catalysts

Nickel-molybdenum catalysts were prepared via the incipient wetness co-impregnation method. The initial contents of MoO_3 and NiO in the catalyst were 15 and 4 wt. %, respectively. The impregnated catalysts were dried in an air flow at 120 ℃ for 2 h and calcined at 425 ℃ for 4 h. The supported catalysts were denoted as NiMo/ASA-Al_2O_3, NiMo/ASA-0.7, NiMo/ASA-0.14, and NiMoASA-0.21, respectively.

2.4. Characterization of catalysts

The BET surface area (S_{BET}), pore size (PS) distribution and pore volume (PV) of the catalysts were measured by conducting nitrogen adsorption/desorption analysis using Micromeritics ASAP 2020 at 77 K. Before the BET analysis, the sample was degassed at 350 ℃ for

8 h. Barret–Joyner–Hallender (BJH) model on the desorption branch was employed to calculate the pore size distribution. The micropore surface area of the catalysts was obtained from the corresponding t-plot.

The XRD patterns of the synthesized catalysts were recorded by a Bruker Advance diffractometer with Da Vinci geometry using the Ni-filtered CuKα radiation (40 kV, 30 mA) instrument. The synthesized catalysts (0.2 g) were ground in a mortar to a particle size of 38 μm. The low angle spectra were recorded to identify changes in the ordering pattern of catalysts ranging from 0.5º to 80º with a step size of 0.01526º and a counting time of 0.4 s per step. By comparing the observed pattern with the diffraction profile reported in the database PDF-4 + ICDD (SiO2-00-058-0344), the qualitative analysis was carried out.

The NH_3-TPD experiments were carried out on a chemisorption physisorption analyzer (ChemBET Pulsar TPR/TPD, Quantachrome) according to the following procedure. First, 200 mg of sample was put into the sample cell and pretreated at 500 ℃ under helium flow rate of 15 mL.min^{-1} for 3 h. After cooling of samples to 100 ℃, the ammonia adsorption was carried out for 40 min under ammonia flow rate of 15 mL.min^{-1}. The physically adsorbed ammonia was removed with blowing helium at 100 ℃ for 2 h. Finally, the NH_3-TPD of the samples was carried out by increasing the cell temperature linearly from 100 to 650 ℃ with a heating rate of 10 ℃.min^{-1} and a helium flow rate of 15 mL.min^{-1}.

The carbonaceous deposit on the spent catalysts was determined using a Pyris TGA1 thermogravimetric analyzer. First, 3 mg samples were heated from 50 to 900 ℃ with a heating rate of 10 ℃.min^{-1} under the air flow rate of 40 mL.min^{-1}. Then the samples were held at isothermal conditions for the initial and final temperatures to allow the stabilization of the catalysts weight. The coke deposits were determined as a difference between weight loss of the fresh and spent carbon-supported catalysts in a region where the coke deposits occurred (300–500 ℃). The carbonaceous deposit on the NMA catalyst was calculated as a difference between the initial stabilized weight and the final stabilized weight. In both cases, the oxidation of MoS_2 and NiS_2 species was considered for calculation of the coke content on the spent catalysts.

2.5. Reaction system for n-hexadecane hydrocracking

The hydrocracking of n-hexadecane was conducted on a steel tubular fixed-bed up-flow reactor. The experimental setup is illustrated in Fig. 1. About 1.0 g catalyst was loaded into the reactor and then was reduced by the H_2 gas at the pressure of 30 bar and a space velocity (Space velocity= flow rate of the reactants / the reactor volume) of 200 h^{-1} with the constant heating rate from ambient to 453 K and maintained at this temperature for 1 h. For preparing NiMoS phases, the catalysts were sulfided by a stream of 1 wt% of dimethyl disulfide in hexane. The sulfidation conditions were under the hydrogen atmosphere with an H_2/Oil volumetric ratio of 80 nl/L, pressure of 30 bar and a space velocity of 200 h^{-1}. Then, the catalyst was sulfided by a stream of 1 wt.% dimethyl disulfide in hexane. The sample was heated from 453 to 633 K with a constant heating rate of 0.5 K.min^{-1} and maintained at this temperature for 10 h. After the activation step, the performance of the catalyst was evaluated for n-C_{16} hydrocracking. The hydrocracking reaction conditions were under the injection rate of 30 cm^3/h, H_2/Oil of 175 nl/L, the pressure of 30 bar, Weight Hourly Space velocity (WHSV) of 3 kg/ (L·h), and Liquid Hourly Space Velocity (LHSV) of 4.2 h^{-1}. The reaction temperature was 573 K. After catalyst testing, the reactor was depressurized under hydrogen flow at 573 K, and after 3 h, the flow was switched to nitrogen and the temperature decreased to room temperature. Liquid products produced during the reaction were analyzed. Data were obtained after at least 24 h in each experimental condition to obtain a stable conversion, product yields, and produced coke.

2.6. Determination of liquid products from n-C_{16} hydrocracking

The liquid products were recovered after each reaction and were analyzed using gas chromatography (GC). An Agilent Technologies 7890A Chromatographer fitted

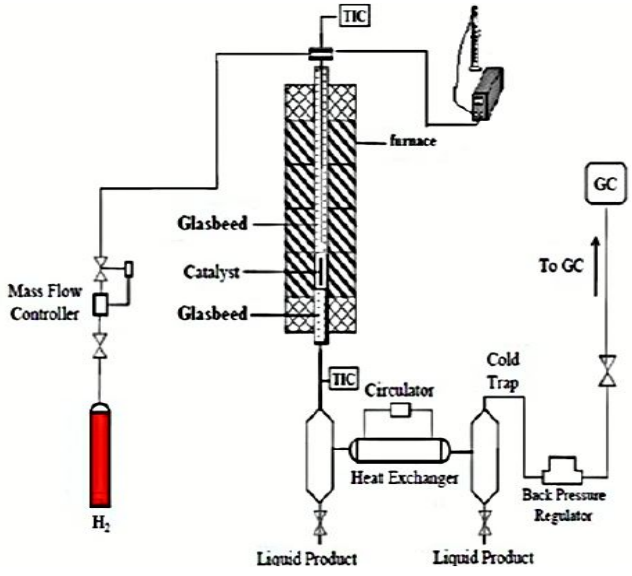

Fig. 1. Schematic of the experimental set up of n-C_{16} hydrocracking using synthesized catalysts.

with a Mass Selective detector (5975C VL MSD with Triple-Axis Detector) was used to measure the amount of each fraction distribution below 230 ℃ in the liquid product. The GC was equipped with a capillary column (Rtx 5 MS, HT-30 m long, 25μm film thickness) and was operated in split mode (split ratio 1:25) with helium as a carrier gas with a flow rate of 1 $mL.min^{-1}$. The data calibration was performed using Agilent MSD Chemstation (Rev E.02.02.1413) to evaluate the percentage of the products. The GC-mass in the steady-state catalytic activity was operated at 60 ℃ for 1.0 min, then a ramp of 10 $℃·min^{-1}$ up to 250 ℃ and the temperature was held up at 250 ℃ for 20 min.

3. Results and Discussion

3.1. Catalyst characterization

The BET surface area, pore size and pore volume of the synthesized catalysts are presented in Table 1. As shown, the prepared catalysts exhibited the high BET surface area which has been classified as mesoporous catalysts. The N_2 Adsorption–desorption isotherms and the corresponding BJH pore size distributions for the NiMo/ASA-Al_2O_3 and NiMo/ASA-0.14 catalysts are shown in Fig. 2. The textural properties of catalysts have been changed by incorporating H_2SO_4 into the support. The loading of H_2SO_4 led to a decrease in the low diameter mesopores. The average pore size was about 87.156, 93.422, 95.325 and 82.996 Å for the NiMo/ASA-0.07, NiMo/ASA-0.14, NiMo/ASA-0.21, and NiMo/ ASA- Al_2O_3 catalysts, respectively. By increasing sulfuric acid content in catalysts, the BET surface area was decreased. a similar trend was reported by Marques *et al.* [14].

As shown in Fig. 2, the shape of N_2 adsorption–desorption isotherm for both catalysts was type IV which revealed the mesoporous structure of synthesized catalysts. The hysteresis loop for NiMo/ASA-Al_2O_3 catalyst can be categorized to H_2 type [15], whereas, the hysteresis loop for the catalyst containing H_2SO_4 exhibited a mixture of cylinder type (H1) of pores [15].

The XRD pattern for the NiMo/ASA-Al_2O_3 catalyst is illustrated in Figure 3. The diffraction peaks for γ-alumina, SiO_2, MoO_3, and Ni_2O_3 phases are observed in the XRD pattern of catalyst. Three diffraction peaks at 2θ = 46, 52, and 66° were assigned to γ- Al_2O_3 [15-18]. The main diffraction peak of SiO_2 was detected at 2θ = 36°. The several diffraction peaks of MoO_3 were observed at 2θ = 23, 27, and 46° [15]. The observed peaks at 2θ = 32.08 and 44.94° could be attributed to the NiO crystalline phase of Ni_2O_3. In the XRD pattern of NiMo/ASA-0.14 catalyst, the γ-alumina, NiO, $NiSO_4$, and MoO_3 phases were detected. The diffraction peaks appeared at 2θ= 37, 46 and 67° were assigned to the γ-Al_2O_3 crystalline phase [15-18]. The main diffraction peak of NiO was detected at 2θ =80 [18]. The diffraction peaks of MoO_3 particles were observed at 2θ = 23 and 27°. The diffraction peak at 2θ = 45° could be attributed to the $NiSO_4$ crystalline phase [15].

The surface acidity of the synthesized catalysts was investigated using NH3-TPD; the results are summerized in Table 2. As shown, each catalyst showed a different distribution of acidic sites. The loadings of sulfate into the NiMo/Al2O3 catalyst significantly changed the structure of acid sites. At low-temperature (260 ℃)the densities of acid site I and at high temperature (420 ℃) the peaks corresponding to acid site II were predominant and related to protonic acidity while at the low-temperature, the acid site I could be attributed to the ammonia coordinated of aluminum species. In this study, the reaction was carried out at the temperature of 300 ℃. Thus, the acid site I should be considered for analysis of acidic properties of catalysts. It was observed that the NiMo/ASA-0.07, NiMo/ASA-0.14, and NiMo/ASA-0.21 catalysts had higher acidities compared with the NiMo/ASA-Al_2O_3 catalyst at the studied condition. Since the cracking function of the NiMo/ASA-Al_2O_3 catalyst was low, the incorporation of electrophilic group (SO_4) into the support was chosen for the treatment of catalyst.

Table 1. Textural properties of catalysts.

Catalyst	Chemical composition (wt. %)				Textural parameter		
	S	Si	Ni	Mo	S_{BET}[a] (m^2/g)	V_{total}[b] (cm^3/g)	d_{avr}[c] (Å)
NiMo / ASA- Al_2O_3	-	47	4	15	244.3946	0.5229	82.996
NiMo / ASA-0.07	0.07	-	4	15	173.4869	0.4267	87.156
NiMo / ASA-0.14	0.14	-	4	15	146.5268	0.3483	93.422
NiMo / ASA-0.21	0.21	-	4	15	113.9732	0.2143	95.325

[a]Specific surface area.
[b]Pore volume.
[c]Average pore size.

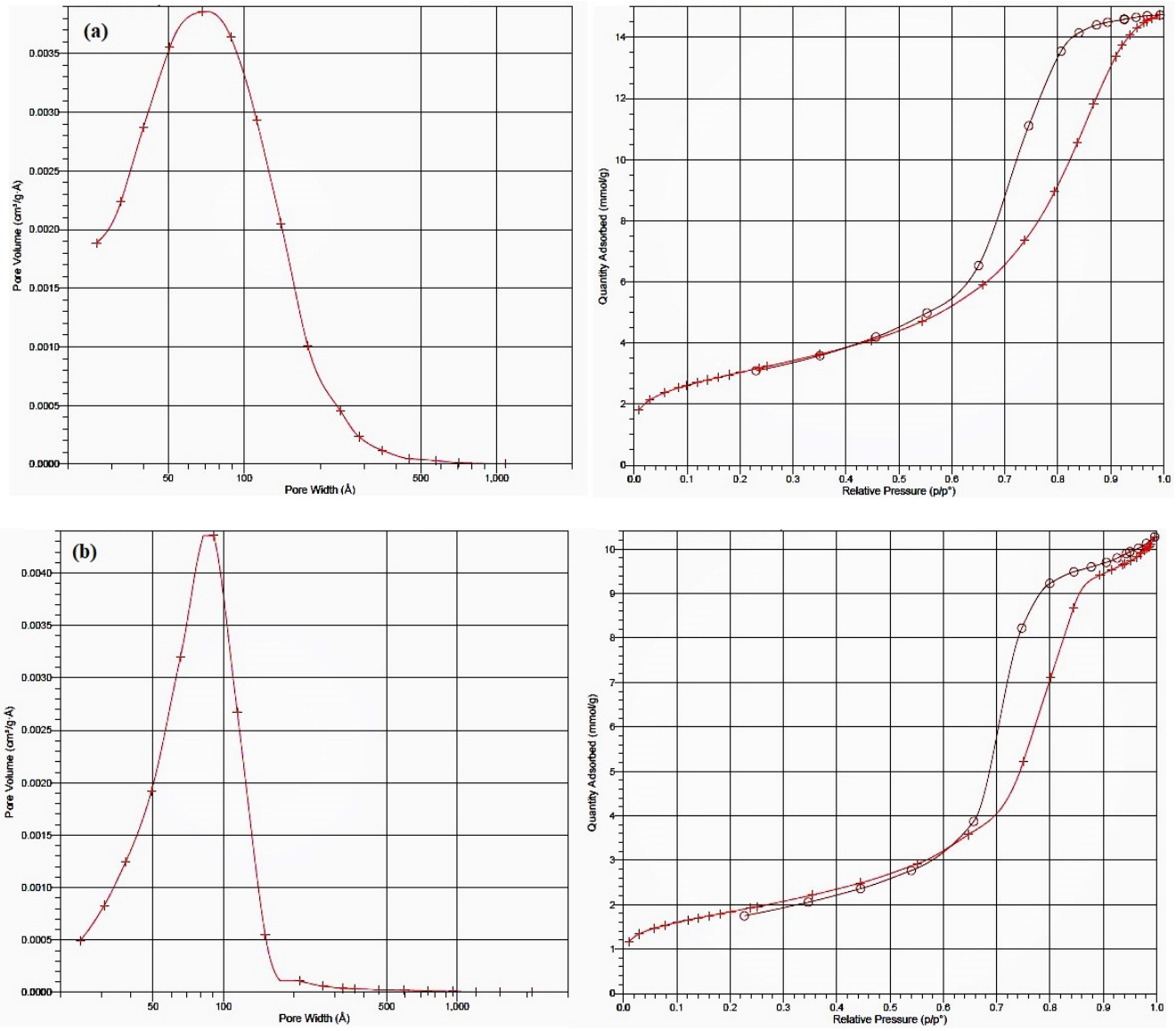

Fig. 2. N_2 adsorption–desorption isotherms and corresponding BJH pore size distributions for the (a) NiMo/ASA-Al_2O_3 catalyst and (b) NiMo/ASA-0.14 catalyst.

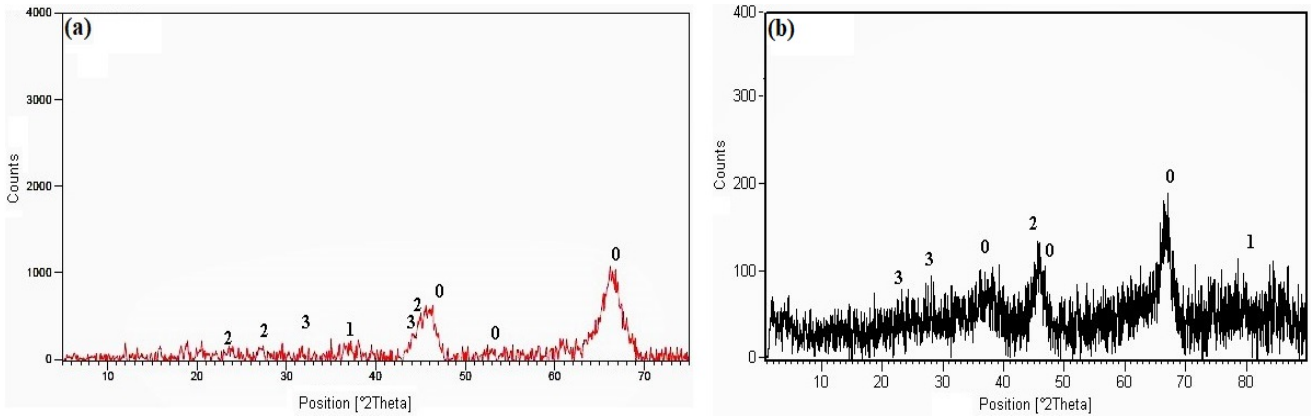

Fig. 3. XRD pattern of NiMo catalyst supported on (a) ASA-Al_2O_3: (0) γ- Al_2O_3, (1) SiO_2, (2) MoO_3, and (3) Ni_2O_3 and (b) NiMo/ASA-0.14: (0) γ- Al_2O_3, (1) NiO, (2) $NiSO_4$, (3) MoO_3

Table 2. Acid Amount of the NiMo/ASA-Al2O3, NiMo/ASA-0.07, NiMo/ASA-0.14, and NiMo/ASA0.21 catalysts.

Catalyst	Acid amount (mmol/g-cat)			
	Acid site I		Acid site II	
	Strength (°C)	Density (mmol/g)	Strength (°C)	Density (mmol/g)
NiMo / ASA- Al2O3	260	0.8861	422	0.6538
NiMo/ ASA-0.07	259	0.9354	416	0.6487
NiMo/ ASA-0.14	254	0.9837	426	0.7314
NiMo/ ASA-0.21	255	0.9954	418	0.7548

The NiMo/ASA-Al_2O_3 catalyst showed the lower acidity which could result in the lower cracking activity. It would be expected that the more acidic catalysts would have a stronger cracking function [19,20].

3.2. Effect of catalyst formulation on the n-hexadecane hydrocracking

The performance of four catalysts NiMo/ASA-Al2O3, NiMo/ASA-0.07, NiMo/ASA-0.14, and NiMo/ASA-0.21 was investigated for n-hexadecane hydrocracking. The catalyst activity for the n-C_{16} hydrocracking has been investigated in the temperature of 573 K with a volumetric H2/hydrocarbon ratio of 175nL/L and total pressure of 30 bar. Table 3 shows the results of hydrocracking process over the NiMo/ASA-Al_2O_3, NiMo/ASA-0.07, NiMo/ASA-0.14, and NiMo/ASA-0.21 catalysts. The total percentages of the products via hydrocracking of n-hexadecane using the synthesized catalysts were also summarized in Table 3.

As shown, the percentage of n-C_{16} hydrocracking to smaller hydrocarbons in presence of the NiMo/ASA catalysts with different sulfuric acid contents was in the range of 91-99%, while the total conversion of n-C_{16} in the presence of the NiMo/ASA-Al_2O_3 was about 94%. The increase in the sulfuric acid content in the NiMo/ASA catalyst resulted in an enhancement in the catalyst activity and the cracking property of the catalyst. The n-C_{16} hydrocracking to the gaseous products has been reduced by increasing the sulfuric acid, and then the liquid products were increased. As shown, the produced gas in the presence of for NiMo/ASA-Al_2O_3 catalyst was higher than that of the other synthesized catalysts, whereas, the yield of produced liquid was the lowest for the NiMo/ASA catalysts. The distribution of the products in the conversion of n-hexadecane for the NiMo/ASA-Al_2O_3 and NiMo/ASA catalysts are illustrated in Fig 4. As shown, the catalyst activity was increased by adding strong acidic sites. The NiMo/ASA catalysts containing various contents of sulfuric acid had more strong acidic sites and few medium acidic sites. Consequently, it could be concluded that the cracking reaction was favorable on strong acidic sites for n-C_{16} hydrocracking under the reaction condition. The sulfuric acid can modify the support morphology (surface area, pore volume, pore size distribution and crystallite phase) which resulted in the formation of the new functional groups on γ-alumina surface. The modified surface properties of γ-alumina support led to the uniform dispersion of Ni and Mo on the support, and this matter increases the quantitative content of acidic sites. It could be concluded that the total number of acidic sites especially the strong acidic sites on the NiMo/ASA catalysts were higher than that of NiMo/ASA-Al_2O_3 catalyst and this resulted in the high conversion of n-C_{16} on Brønsted acid sites [21,22].

Table 3. Total percentage of the products using the NiMo/ASA-Al_2O_3, NiMo/ASA-0.07, NiMo/ASA-0.14, and NiMo/ASA-0.21 catalysts.

Catalyst	Conversion (%)[a]	Gaseous products (%)	Liquid products (%)
NiMo / ASA- Al_2O_3	93.98	19.82	80.18
NiMo / ASA-0.07	91.45	12.26	87.74
NiMo / ASA-0.14	97.86	15.37	84.63
NiMo / ASA-0.21	98.61	18.64	81.36

[a] $\%\ total\ conversion = \frac{mass\ change\ of\ feed}{primary\ mass\ of\ feed} \times 100 = \frac{primary\ feed - the\ rest\ of\ the\ feed}{primary\ mass\ of\ feed} \times 100$

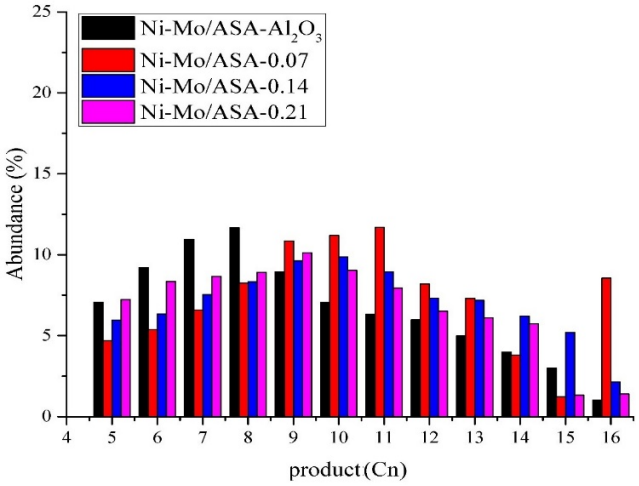

Fig. 4. Distribution of the products in the conversion of n-hexadecane for the NiMoASA and NiMo/ASA-Al_2O_3 catalysts.

One of the most important advantages of the use of uniform dispersion of NiMo catalyst on the support for the conversion of heavy feed stocks is the inhibition of the coke formation [22]. The coke deposition content on the catalyst surface during n-C_{16} hydrocracking is presented in Table 4. The coke formation on the catalyst and catalyst deactivation could be affected by the catalyst activity [23]. The polymerization of n-C_{16} and products could be resulted in the coke formation. Since coke can cover the active sites for hydroprocessing reactions, the coke formation could deactivate the catalyst efficiency after a while [23]. The results proved that the isomerization rate in the presence of the sulfated catalyst was lower than that of the unsulfated catalyst. The deactivation of catalyst was decreased in the presence of sulfated catalyst and the hydrocracking of n-C_{16} was increased. The higher content of sulfuric acid in the support matrix resulted in the more cracking power of the catalyst.

The conversion of n-paraffins have occurred using three competitive reactions and the isoparaffin was almost formed as a primary product via the hydro-isomerization of the n-alkane [24]. Particularly, the reaction temperature and the chain length can change the hydro-isomerization selectivity, isomerization/cracking rates and activation energies through the different reaction pathways [24]. Since the cost of the sulfuric acid is much lower than that of the silica, it could be concluded that the use of sulfuric acid can be considered as an optimal factor for increasing the acidity and the hydrocracking capacity of the catalyst for conversion of the large molecules into low molecular weight fractions.

4. Conclusions

The n-hexadecane hydrocracking has been studied in a downstream fixed-bed continuous flow reactor using synthesized catalysts with different sulfuric acid contents. The results indicated that the catalyst acidity was increased when sulfuric acid content of the catalysts structure increased. The cracking reaction in the presence of the sulfided-catalyst was more than that of the NiMoSA catalyst. The use of sulfuric acid as an electrophilic group in the catalyst structure for production of low molecular weight fractions via hydrocracking process could be an economic and optimum option to increase the catalyst activity.

Table 4. Coke deposition content on the NiMo/ASA-Al_2O_3, NiMo/ASA-0.07, NiMo/ASA-0.14, and NiMo/ASA0.21 catalysts.

Catalyst	Coke (g coke/ g cat.)
NiMo / ASA- Al_2O_3 spent	0.0087
NiMo / ASA-0.07 spent	0.0059
NiMo / ASA-0.14 spent	0.0032
NiMo / ASA-0.21 spent	0.0029

References

[1] C. Leyva, J. Ancheyta, A. Travert, F. Maugé, L. Mariey, J. Ramírez, M.S. Rana, Appl. Catal. A 425–426 (2012) 1-12.
[2] W. Li, J. Zhu, J. Qi, J. Fuel Chem. Technol. 35 (2007) 176–180.
[3] J. Ancheyta, M. S. Rana, Future technology in heavy oil processing, Conference Proceedings.
[4] E. M. Juárez, F. J. O. García, P. S. Hernández, Fuel 135 (2014) 51–54.
[5] J. G. Speight, Catal. Today 98 (2004) 55–60.
[6] P.P. Dik, O.V. Klimov, G.I. Koryakina, K.A. Leonova, V.Y. Pereyma, S.V. Budukva, E.Y. Gerasimov, A.S. Noskov, Catal. Today 220–222 (2014) 124–132.
[7] J. Mosio-Mosiewski, I. Morawski, Appl. Catal. A 283 (2005) 147–155.
[8] J.M. Schweitzer, S. Kressmann, Chem. Eng. Sci. 59 (2004) 5637–5645.
[9] H. Fan, Z. Li, T. Liang, J. Fuel Chem. Technol. 35 (2007) 32–35.

[10] C. Dujardin, M.A. Lélias, J. van Gestel, A. Travert, J.C. Duchet, F. Maugé, Appl. Catal. 322 (2007) 46–57.
[11] J.-S. Choi, F. Maugé, C. Pichon, J. Olivier-Fourcade, Appl. Catal. A 267 (2004) 203–216.
[12] S. G. A. Ferraz, B. M. Santos, F. M. Z. Zotin, L. R. R. Araujo, J. L. Zotin, Ind. Eng. Chem. Res. 54 (2015) 2646-2656.
[13] S. G. A. Ferraz, F. M. Z. Zotin, L. R. R. Araujo, J. L. Zotin, Appl. Catal. A 384 (2010) 51–57.
[14] J. Marques, D. Guillaume, I. Merdrignac, D. Espinat, S. Brunet, Appl. Catal. B 101 (2011) 727–737.
[15] P. Y. Looi, A. R. Mohamed, C. T. Tye, Chem. Eng. J. 181–182 (2012) 717–724.
[16] Y. Kim, C. Kim, P. Kim, J. Yi, J. Non-Cryst. Solids 351 (2005) 550–556.
[17] M. May, J. Navarrete, M. Asomoza, R. Gomez, J. Porous Mater. 14 (2007) 159–164.
[18] Q. Yuan, A.-X. Yin, C. Luo, L.-D. Sun, Y.-W. Zhang, W.-T. Duan, H.-C. Liu, C.-H. Yan J. Am. Chem. Soc. 130 (2008) 3465–3472.
[19] M. A. Ali, T. Tatsumi, T. Masuda, Appl. Catal. A 233 (2002) 77–90.
[20] R. G. Tailleur, Stud. Surf. Sci. Catal. 143 (2000) 321-329.
[21] V. B. Phapale, M. Guisán-Ceinos, E. Buñuel, D. J. Cárdenas, Chem. Eur. J. 15 (2009) 12681–12688.
[22] N. Panariti, A. Del Bianco, G. Del Piero, M. Marchionna, Appl. Catal. A 204 (2000) 203–213.
[23] T. Olorunyolemi, R.A. Kydd, Catal. Lett. 63 (1999) 173–178.
[24] V. Calemma, S. Peratello, C. Perego, Appl. Catal. A 190 (2000) 207–218.